

**Abstract.** This paper presents a fundamental numerical analysis of flow and heat transfer in a vertical rotating disk reactor. These reactors are commonly used for growing thin films *via* chemical vapor deposition. Under certain conditions, rotating disk reactors have been found to exhibit multiple steady states, where desirable and undesirable flow patterns co-exist at the same conditions. The focus of this research is to predict the onset of multiplicity with respect to key system parameters, and thereby give guidance on reactor design and operation. Using bifurcation analysis algorithms we directly track what we believe is a global stability limit (the onset of multiple solutions). Results for a model system with constant physical and transport properties along with the Boussinesq approximation are compared to a model with actual fluid properties for nitrogen gas coupled with the ideal gas law.

## 1 INTRODUCTION

This paper represents a fundamental bifurcation analysis of stagnation flows in a vertical rotating-disk reactor (RDR). The objective is to map out regions of parameter space where a RDR may exhibit erratic behavior. Since the behavior is caused by multiple steady states or periodic motion the onset of multiplicity is tracked through bifurcation and stability analysis. Using this data, we provide a correlation between dimensionless groups that can be used to design reactors that operate in regions of parameter space where a single steady state exists.

Metalorganic vapor phase epitaxy (MOVPE) has become the method of choice in manufacturing complex heterostructures for the next generation of optoelectronic devices [1, 2, 3]. Advanced multi-layered structures such as vertical-cavity surface-emitting lasers (VCSELs) and quantum cascade lasers require strict control over the growth process [4]. Hundreds of thin layers (on the order of Ångstroms) must be grown one on top of the other with uniform thickness and composition. This requires a robust process with minimal variation between alternating layers and from run to run. Vertical RDRs are currently the leading choice for production due to their high throughput, scalability, and versatility. However, improper design and/or operation of RDRs can lead to unreliable performance and, ultimately, device failure.

The cause of the erratic behavior in RDRs can be traced to bifurcation phenomena. It has been demonstrated that both multiple steady states and periodic flows can exist in RDRs [5, 6, 7]. When multiple steady states are present, the flow pattern can settle on a steady state very different from the traditional stagnation flow pattern described by the von Karman similarity solution for a rotating disk [8]. These flow patterns can generate flow recirculations or temperature oscillations near the deposition surface. This damages film quality by introducing nonuniform film thickness and/or composition. A robust reactor design should eliminate the possibility of operating in regions where multiplicity exists. This paper shows how bifurcation analysis algorithms can be used to

$$\begin{aligned} \text{Total Mass:} & \quad \nabla \cdot (\rho \mathbf{u}) = 0 \\ \text{Momentum:} & \quad \rho \mathbf{u} \cdot \nabla \mathbf{u} = -\nabla P + \nabla \cdot \left[ \mu \nabla \mathbf{u} + \mu (\nabla \mathbf{u})^T - (2/3) \mu \mathbf{I} (\nabla \cdot \mathbf{u}) \right] + \rho \mathbf{g} \\ \text{Energy:} & \quad \rho C_p (\mathbf{u} \cdot \nabla T) = \nabla \cdot (k_g T) \end{aligned}$$

Table 1: Fundamental Conservation Equations

efficiently derive RDR design criteria that demarkate multiplicity in a specific reactors parameter space.

There are several possible stability limits to the Karman-like flows. Below a critical value of the Rayleigh number,  $Ra_{lin}$ , we expect this flow to be linearly stable. Calculations indicate that this flow goes unstable in an oscillatory manner. However, it is possible that this flow could be linearly stable, but be unstable to large enough disturbances. This sort of behavior could be especially annoying in a production facility, because it could cause the reactor to run well for long periods of time, but to occasionally give erratic behavior. We hypothesize that there is a second stability limit  $Ra_{global}$  such that for Rayleigh numbers below this, the reactor will approach the Karman-like solution no matter how much it is disturbed. It is very plausible that this global stability limit is the Rayleigh number,  $Ra_{mult}$ , at which multiple steady state solutions first appear. Using bifurcation tracking algorithms it is possible to track  $Ra_{mult}$  (and by our hypothesis  $Ra_{global}$ ) as a function of the Reynolds number.

This analysis uses an axisymmetric 2D flow and heat transfer model of a RDR. A simple model based on constant physical and transport parameters is first used for elucidating the relationships/scaling laws between various design parameters in terms of dimensionless groups. The results of a more realistic model typical of that used in simulating MOVPE systems are then compared against the simple model. The simple model can clearly demonstrate underlying relationships/scaling laws that the realistic model tends to mask. The resulting diagrams can be applied to the design and operation of RDRs to point out when multiple steady states are possible, leading to undesired behavior.

## 2 MODEL DEFINITION

The models are based on the fundamental conservation equations for momentum and heat transfer shown in Table 1. Two variations of the model are used, a simple model and a realistic model. The simple model solves the fundamental equations with constant material properties and applies the Boussinesq approximation for density variation: the density is constant in the fundamental equations except for the body force term in the momentum equation,  $\rho \mathbf{g}$ , which is replaced with a first order approximation,  $\rho_o \mathbf{g} \beta \Delta T$ . The realistic model solves the fundamental equations in Table 1 with variable material properties and includes the ideal gas law for density variation. The realistic model is the standard formulation used for modeling MOVPE systems [9].

The resulting set of coupled PDEs are solved simultaneously using the code MPSalsa developed by Sandia National Laboratories [10, 11]. MPSalsa was designed to solve low-Mach number incompressible flows in two- and three-dimensions using a Galerkin/least-squares finite element formulation on massively parallel architectures [12]. The material properties of the fluid in the realistic model are provided by calls to the TRANFIT [13] and CHEMKIN [14] libraries. The nonlinear problem is solved directly to steady-state using fully-coupled Newton-Krylov solver [15]. The resulting linear systems are solved iteratively using domain decomposition preconditioners and the GMRES method as implemented in the Aztec package [16].

Steady-state solution branches are tracked as a function of a parameter using a pseudo arc-length continuation algorithm [17]. A turning point (fold) tracking algorithm is used to locate the bifurcation points by continuing in the first parameter while computing a corresponding second

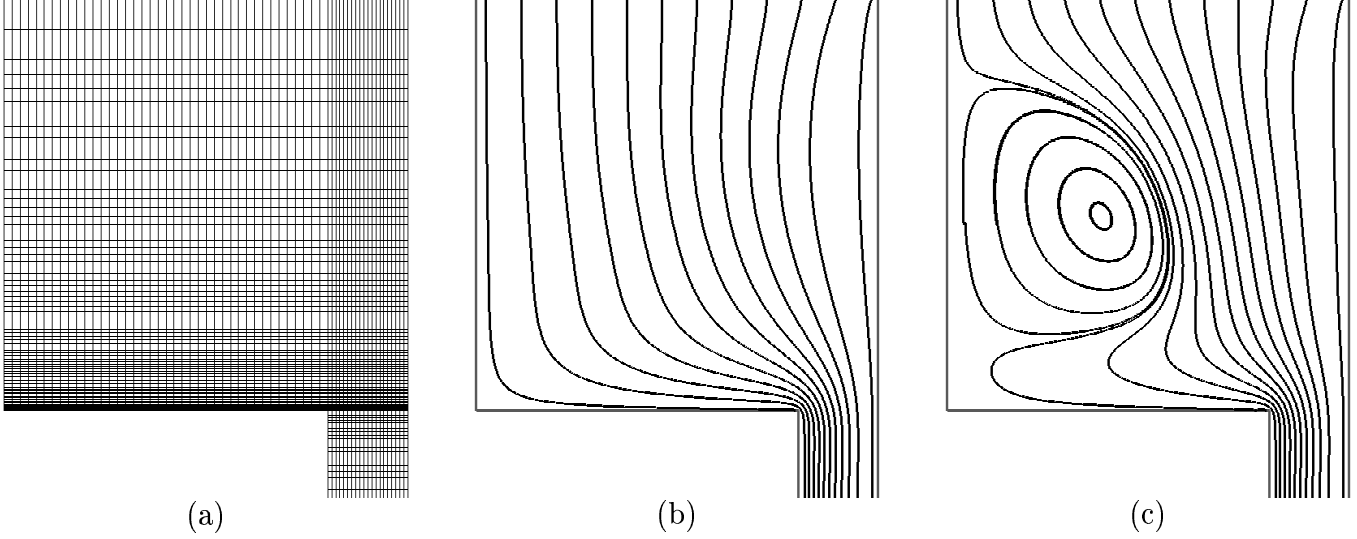


Figure 1: 2D Axisymmetric mesh and streamlines for the stable solution branches:  $Re = 92$ ,  $P = 0.1$  atm,  $T_{susceptor} = 373.5$  K,  $V_{inlet} = 3.55$  cm/s. (a) mesh, (b) desired solution, (c) undesired solution

parameter. The bifurcation points signify the beginning of multiplicity in this reactor. These algorithms are implemented in the LOCA library [18] developed by Sandia National Laboratories, which has been linked to the MPSalsa code.

The reactor in this paper is assumed to be axially symmetric, thus reducing to two dimensions in cylindrical coordinates. The finite element mesh is shown in Figure 1a. The mesh consists of 5580 bilinear finite elements corresponding to 6075 nodes and 30375 unknowns. The five dependent variables are the radial, axial and azimuthal velocities and the temperature and hydrodynamic pressure. Pure nitrogen is used as the carrier gas in the realistic model. The simple model is solved in dimensionless form and thus needs no carrier gas specification. The gas enters through the top surface with uniform velocity and temperature profiles. The walls are water cooled and the susceptor is held at a uniform temperature.

Figure 1b depicts the streamlines in a RDR for the desired stagnation flow pattern that can yield excellent film uniformities. Figure 1c depicts a second stable steady state at the same operating conditions with a detrimental flow pattern. A buoyancy-induced flow recirculation forms over the deposition surface causing steep radial gradients, destroying film uniformity.

### 3 DIMENSIONAL ANALYSIS

The models are characterized in dimensionless form by the Rayleigh number,  $Ra$ , and the rotational Reynolds number,  $Re$ . The dimensionless numbers are defined as:

$$Re = \frac{\omega R_i^2}{\nu} \quad Ra = \frac{g\beta\Delta T\delta^2 R_i}{\alpha\nu} = \frac{g\beta\Delta T R_i}{\alpha\omega} \quad (1)$$

While these quantities are well-defined in the simple model, there is a choice in the realistic model as to what temperature is used to evaluate the properties. In this work we evaluate all properties at the cold inlet temperature because we have found this choice to give the best agreement between the simple and realistic models.

The parameter space of RDRs is quite large. To reduce the number of parameters we set the inlet velocity as a function of the rotation rate such that “good” uniformity is maintained. Good uniformity in this case is for a transport limited deposition system. This condition linking the inlet velocity to rotation rate yields an acceptable estimate of uniformity but does not represent the best achievable uniformity. The condition eliminates the need to perform a bifurcation analysis over the

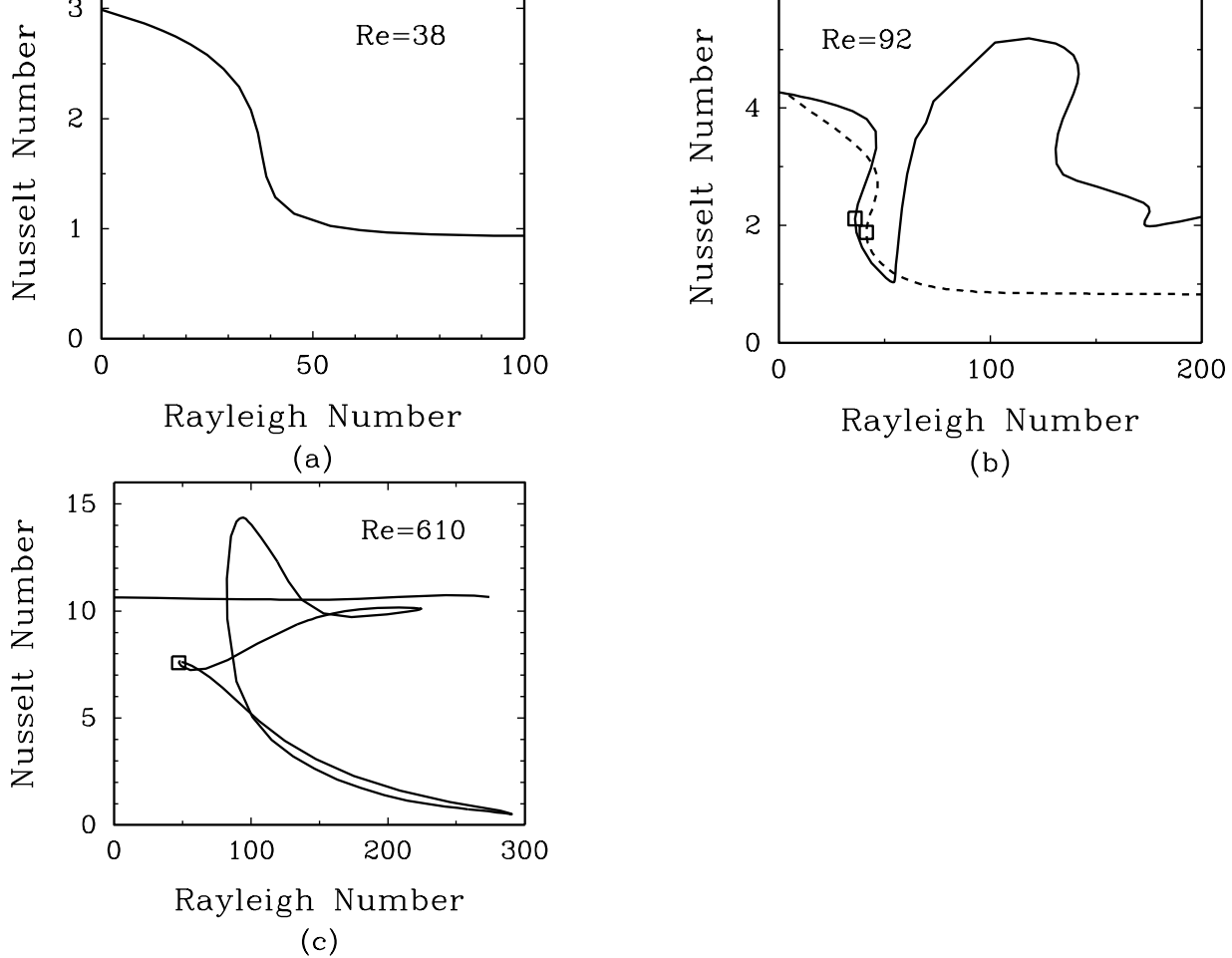


Figure 2: Bifurcation diagrams depicting the various phenomena observed in a RDR. (a) continuous transition  $Re = 38$ , (b) fold (hysteresis)  $Re = 92$ , (c) disconnected branches (horizontal branch and isola)  $Re = 610$ . All three behaviors have been observed in the simple model (solid line) while continuous transitions and folds have been observed in the realistic model (dashed line) under typical operating conditions.

entire range of inlet velocities and rotation rates. The inlet velocity correlation to susceptor rotation rate is based upon the 1D model of a heated, rotating disk developed by Evans and Greif [19] (an extension to the von Karman similarity solution [8] to include heat transfer). The similarity solution predicts that the boundary layer above the disk is on the order of  $\delta = \sqrt{\nu/\omega}$ . This type of solution is highly desirable since the temperature and axial velocity are functions of the axial coordinate only. This tends to produce uniform deposition across the susceptor. The similarity solution shows that when an infinite disk spins at a frequency  $\omega_o$  the axial velocity far from the disk approaches the value [19]:

$$u_z \rightarrow u_{z_o} = 0.885\sqrt{\omega_o\nu} \quad (2)$$

This velocity is referred to as the matched velocity (i.e. matched to the rotation rate to produce good uniformity over the susceptor). This is the velocity a spinning disk naturally induces far away from the disk. In using the matched velocity, we assume that the radius of the susceptor and the distance between gas inlet and susceptor are much larger than  $\delta$ .

## 4 CONTINUATION STUDIES

In this section we will present results of pseudo arc-length continuation runs that are used to detect

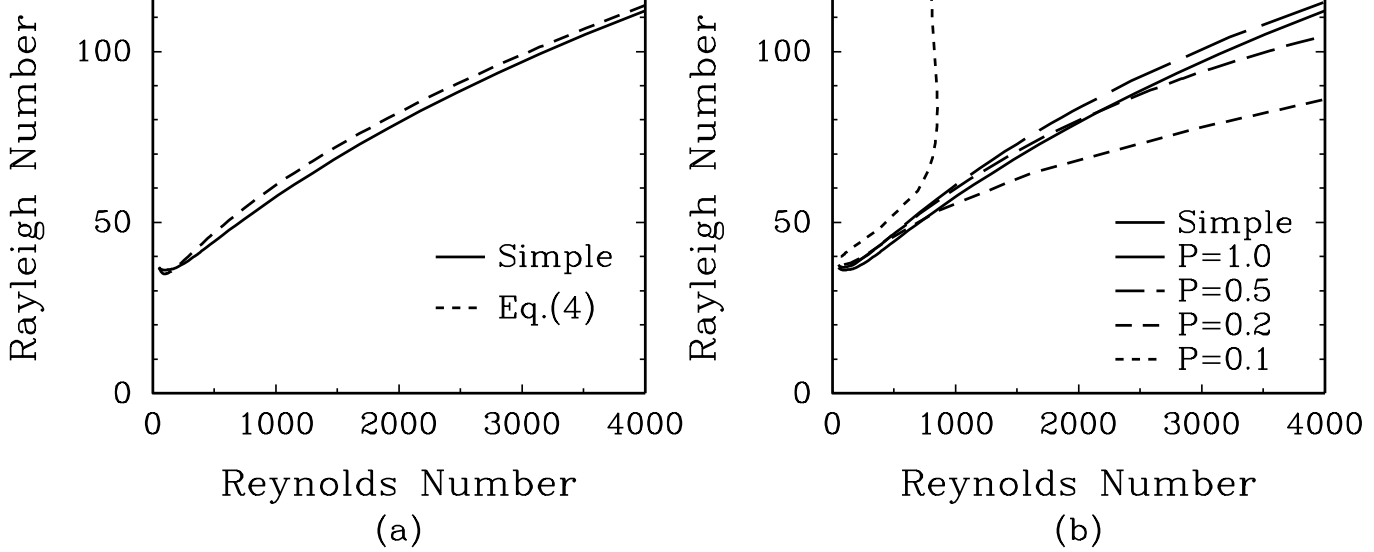


Figure 3: Parameter plot of the locus of bifurcation points signaling the onset of multiplicity. Parameter plot comparing the simple model and the realistic model at various pressures.

the onset of multiplicity (i.e. the global stability limit). In all cases, the rotation rate of the disk (as measured by  $Re$ ) is held fixed, as is the inlet velocity (specified by Eq. 2) and the reactor geometry. Steady-state solutions are tracked as a function of the temperature of the susceptor, which controls the destabilizing buoyancy force (as measured by  $Ra$ ). The results of the continuation runs for both the simple and realistic models are shown in Figure 2. The Nusselt number,  $Nu$ , at the center of the disk is used to characterize the solution:

$$Nu = \frac{H}{\Delta T} \left. \frac{\partial T}{\partial z} \right|_{r=0} \quad (3)$$

A convective roll cell such as that seen in Figure 1c results in a decreased value of  $Nu$ . The three runs for the simple model show three qualitatively different behaviors. At  $Re = 38$  the transition from desirable to undesirable flow occurs continuously at around  $Ra = 30$ . At  $Re = 92$ , the transition is discontinuous with the familiar S-shaped curve symbolizing a region of hysteresis. The realistic model (dashed line) calculated at a pressure of 0.1 atm agrees very well with the simplistic model at low Rayleigh numbers. At  $Re = 610$ , the curve is qualitatively different, with the horizontal branch coexisting with an isola (a closed loop of solution branches). In both the  $Re = 92$  and  $Re = 610$  cases, one can avoid even the possibility of undesirable recirculations by designing the reactor to operate where there is no multiplicity. This can be achieved by designing the reactor to operate at a value of  $Ra$  below the turning point, which is marked with the box symbol. (This conclusion assumes that there are no other solution branches at these low values of  $Ra$ , which we can argue on physical grounds but not prove).

## 5 PARAMETER TRACKING

In this section we extend the results found in the previous section to large ranges of  $Re$  by directly tracking the turning points that signal the onset of multiplicity. Figure 3a presents the locus of this turning point for the simple model. The dashed line is a simple curve fit that approximates this line:

$$Ra = 1.75Re^{0.5}(1 + 100/Re) \quad (4)$$

Note that for large disk spin rates  $Re$ , the onset of multiplicity is independent of any reactor length scale, only being dependent on the boundary layer thickness  $\delta$ .

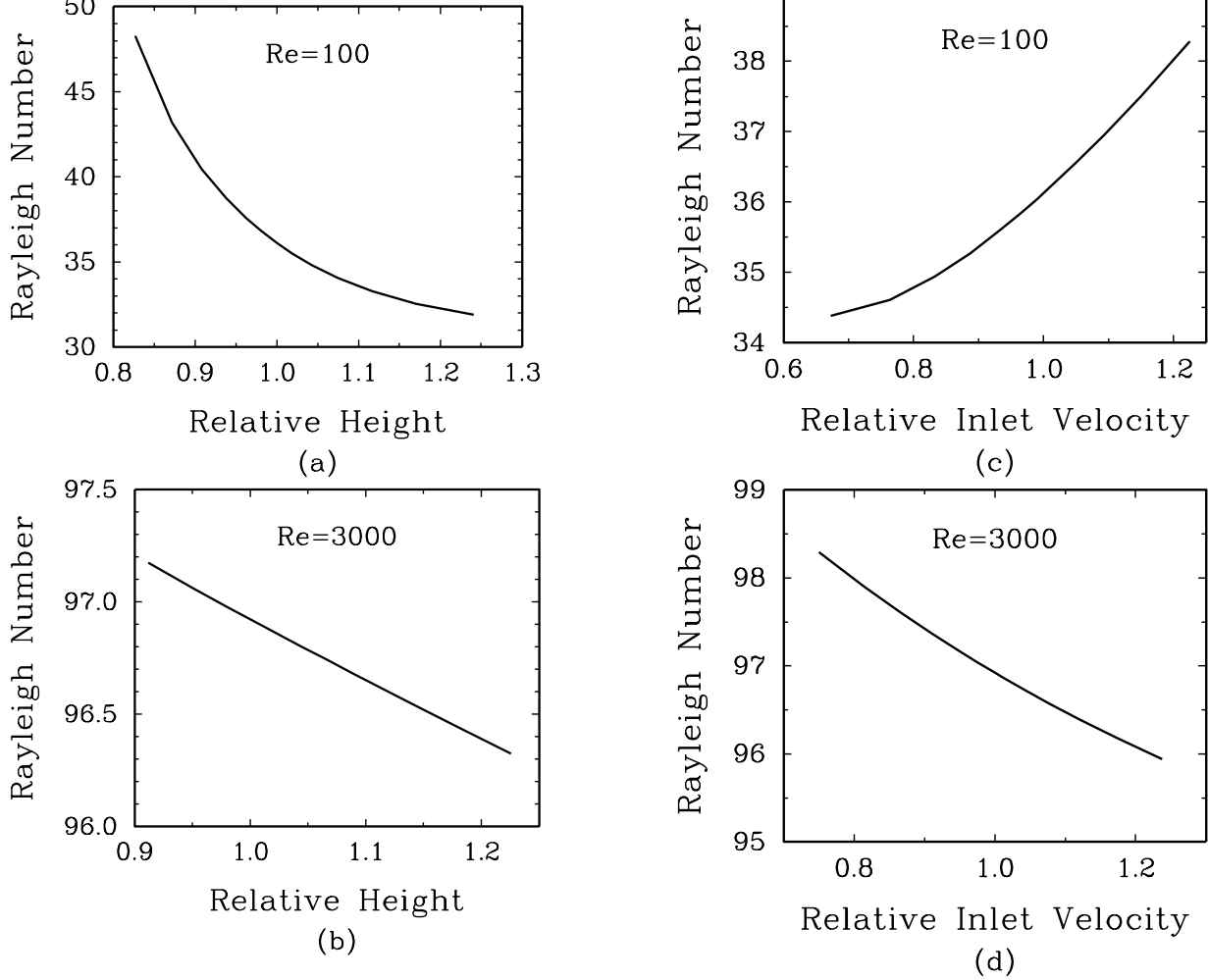


Figure 4: Variation of bifurcation point in  $Ra$  with respect to the relative height and inlet velocity (compared to the standard values) for various  $Re$ .

In Figure 3b the same turning point curve is plotted with turning point calculations for the realistic model. At low pressure of  $P = 0.1$  atm, the realistic model agrees well with the simple model up to  $Re = 700$  when the physical properties in the definitions of  $Re$  and  $Ra$  are evaluated at the cold inlet temperature. When evaluated at the average temperature between the inlet and susceptor temperatures, the locus of turning points does not approximate the results of the simple model. At  $P = 1.0$  atm, where large  $Ra$  can be achieved with smaller temperature differences, the realistic model agrees very well with the simple model. At  $P = 0.5$  and  $P = 0.2$  the fit is close, but diverges as higher susceptor temperatures are required to attain the corresponding Rayleigh numbers. Large temperature differences cause the discrepancy between the models due to the application of the Boussinesq approximation.

To further generalize the results, we investigate the sensitivity of the correlation in Eq. 4 to two additional parameters: the height of the reactor,  $H$ , and the inlet velocity (i.e. sensitivity to deviations in the matched velocity),  $u_{z_o}$ . The sensitivity was checked at  $Re = 100$  and  $Re = 3000$ , where different terms in the fundamental equations dominate. The results are shown in Figure 4, where the  $Ra$  of the turning point is shown to vary as a function of  $H$  and  $u_{z_o}$  compared to their standard values. The results show that at low  $Re$ , there is a strong inverse relationship with  $H$  and a weaker positive relationship with  $u_{z_o}$ . For the large  $Re$  case, the turning point is rather insensitive to the inlet position and velocity.

Numerical simulation of coupled flow and heat transfer and the use of bifurcation analysis algorithms have been applied to the rotating disk CVD reactor. Regions of solution multiplicity, where a desirable von Karman-like solution and an undesirable buoyancy-driven flow solution can coexist, are found. A line in design space symbolizing the onset of solution multiplicity, and therefore the possibility of undesirable convective flow cells, is directly calculated. For a simplistic model of constant physical properties, this line is fit by a two-term scaling law. Comparisons with a more realistic model, with temperature-dependent physical properties, show that the simple model holds for moderate temperature variation. Results not shown here also indicate that evaluating dimensionless quantities at the cold inlet temperatures produced the best results in comparisons to the simple constant-property model.

## References

- [1] P. Grodzinski, S. P. DenBaars, and H. C. Lee. From research to manufacture - the evolution of MOCVD. *Journal of Materials*, pages 25–32, December 1995.
- [2] T. F. Kuech and N. R. Perkins. Metalorganic vapor phase epitaxy of II-VI materials for visible light emitters. *Journal of Crystal Growth*, 166:558–565, 1996.
- [3] A. G. Thompson. Materials update, MOCVD technology for semiconductors. *Materials Letters*, 30:255–263, 1997.
- [4] S. Pellegrino and L. Tarricone. MOVPE growth and study of InP-based materials: opportunities and challenges. *Materials Chemistry and Physics*, 66(2-3):189–196, Oct 2000.
- [5] K. F. Jensen, D. I. Fotiadis, and T. J. Mountziaris. Detailed models of the MOVPE process. *Journal of Crystal Growth*, 107:1–11, 1991.
- [6] R. B. Lehoucq and A. G. Salinger. Massively parallel linear stability analysis with P\_ARPACK for 3D fluid flow modeled with MPSalsa. *Lecture Notes in Computer Science*, 1541:286–295, 1998.
- [7] H. Van Santen, C. R. Kleijn, and H. E. A. van den Akker. On multiple stability of mixed convection flows in a chemical vapor deposition reactor. *Int. J. Heat and Mass Transfer*, 44:659–672, 2001.
- [8] H. Schlichting. *Boundary-Layer Theory*. McGraw-Hill, 1968.
- [9] D. Fotiadis, S. Kieda, and K. F. Jensen. Transport phenomena in vertical reactors for metalorganic vapor phase epitaxy I. effects of heat transfer characteristics, reactor geometry, and operating conditions. *Journal of Crystal Growth*, 102:441–470, 1990.
- [10] J. N. Shadid, H. K. Moffat, S. A. Hutchinson, G. L. Hennigan, K. D. Devine, and A. G. Salinger. MPSalsa: A finite element computer program for reacting flow problems - Part I theoretical development. Technical report, Sandia National Laboratories, Albuquerque, New Mexico 87185, 1996. SAND95-2752.
- [11] A. G. Salinger, K. D. Devine, G. L. Hennigan, H. K. Moffat, S. A. Hutchinson, and J. N. Shadid. MPSalsa: A finite element computer program for reacting flow problems - part II user's guide. Technical report, Sandia National Laboratories, Albuquerque, New Mexico 87185, 1996. SAND96-2331.

- [12] J. N. Shadid, S. A. Hutchinson, G. L. Henningan, H. K. Mollat, K. D. Devine, and A. G. Salinger. Efficient parallel computation of unstructured finite element reacting flow solutions. *Parallel Computing*, 23:1307–1325, 1997.
- [13] R. J. Kee, G. Dixon-Lewis, J. Warnatz, M. E. Coltrin, and J. A. Miller. A fortran computer code package for the evaluation of gas-phase, multicomponent transport properties. Technical report, Sandia National Laboratories, Albuquerque, New Mexico 87185, 1986. SAND86-8246.
- [14] R. Kee, F. M. Rupley, E. Meeks, and J. A. Miller. Chemkin-III: A fortran chemical kinetics package for the analysis of gas-phase chemical and plasma kinetics. Technical report, Sandia National Laboratories, Albuquerque, New Mexico 87185, 1996. SAND96-8216.
- [15] J. N. Shadid, R. S. Tuminaro, and H. F. Walker. An inexact newton method for fully-coupled solution of the navier-stokes equations with heat and mass transport. *J. Comput. Phys.*, 137:155–185, 1997.
- [16] S. A. Hutchinson, J. N. Shadid, and R. S. Tuminaro. Aztec user’s guide: Version 1.0. Technical report, Sandia National Laboratories, Albuquerque, New Mexico 87185, 1995. SAND95-1559.
- [17] H. B. Keller. Numerical solution of bifurcation and nonlinear eigenvalue problems. In P. H. Rabinowitz, editor, *Applications of Bifurcation Theory*, pages 159–384. Academic Press, New York, 1977.
- [18] A. G. Salinger, L. A. Romero, R. P. Pawlowski, E. D. Wilkes, and E. A. Burroughs. LOCA: A library of continuation algorithms - Theory manual and user’s guide. Technical report, Sandia National Laboratories, Albuquerque, New Mexico 87185, 2001. SAND01-XXXX.
- [19] G. H. Evans and R. Greif. Forced flow near a heated rotating disk: A similarity solution. *Numerical Heat Transfer*, 14:373–387, 1988.

Paper: C17

Title: Computational Design and Analysis of MOVPE Reactors

Authors:

R.P. Pawlowski  
Computational Sciences Department  
Sandia National Laboratories  
Albuquerque, NM 87185

A.G. Salinger  
Computational Sciences Department  
Sandia National Laboratories  
Albuquerque, NM 87185

L.A. Romero  
Computational Math and Algorithms Department  
Sandia National Laboratories  
Albuquerque, NM 87185

J.N. Shadid  
Computational Sciences Department  
Sandia National Laboratories  
Albuquerque, NM 87185